# Automatic Tuning of Attitude Control System for Unmanned Aerial Vehicles

Liuping Wang, Pakorn Poksawat, Xi Chen and Abdulghani Mohamed

School of Engineering, RMIT University, Melbourne, Australia

# Outline

# Motivations

### Applications

Unmanned Aerial Vehicles (UAVs) have become very popular in the last decade in both military and civilian applications:

- surveying dangerous or complex terrains, localization and mapping;
- localization and mapping.

### Control

A robust attitude control system is required to enable safe and stable flight in most indoor/outdoor applications.

# Popular control strategy

Proportional-Integral-Derivative (PID) controllers have become one of the most widely used controllers in autopilots due to

1. its simplicity and low computational intensity;
2. easiness to be understood by engineers;
3. reliability in implementation.

# Challenges

### Crash UAVs

When selecting the PID controller parameters by the trial and error process, it is easy to crash the UAV because it is a unstable system.

### Time consuming

There are six PID controllers in cascade structures for a typical flight controller. This leads to high demanding of manpower and increased cost.

# Automatic Tuning of PID Controllers

- Automatically find the mathematical model of the plant to be controlled;
  - identification experiment design to ensure the collection of input and output data contains useful information for controller design;
  - closed-loop system is required to be stable for safety of equipment during the experiments;
  - identification experiments need to be simple and easy to execute.
- Automatically determine the controller parameters with minimum human intervention.

# Outline

# Presentation Outline

## Dynamics of UAVs

- Quadrotor
- Hexacopter
- Fixed wing micro-aircraft

## Automatic controller tuning

- Relay feedback control
- Estimation of plant frequency information
- PID controller design

## Experimental and flight testing results

- Quadcopter
- Hexacopter
- Fixed wing micro-aircraft

# Multi-rotor UAVs

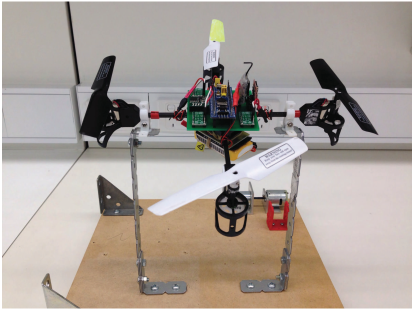

(a) Quadrotor

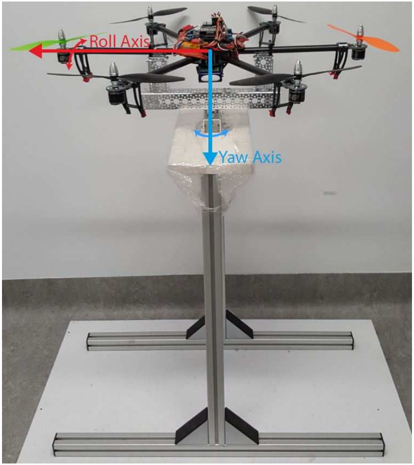


(b) Hexacopter

Figure: Unmanned aerial vehicles (multi-rotor)

# Fixed-wing UAV

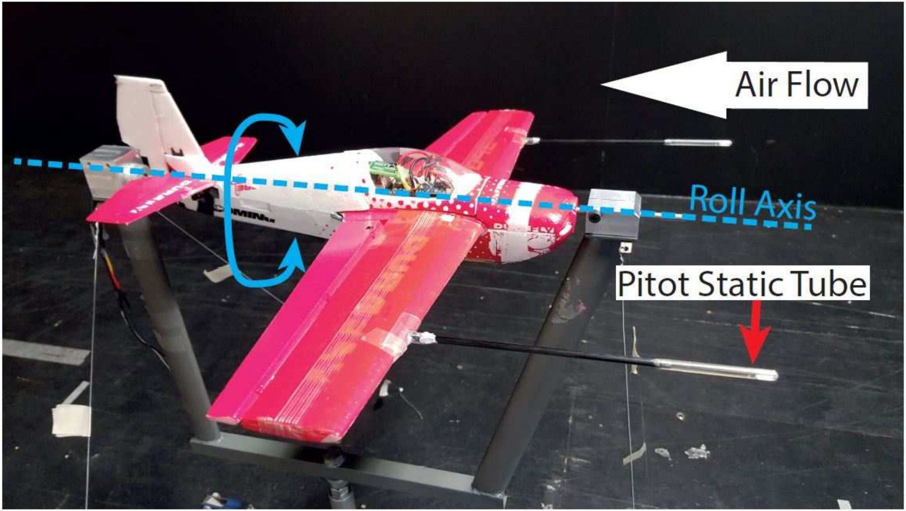


Figure: Fixed-wing micro-aircraft

# Outline

# Inertial Frame and Body Frame (i)

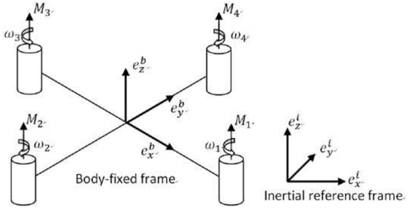


(a) Quadrotor

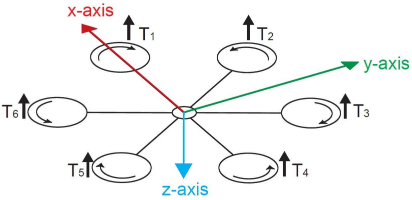


(b) Hexacopter

Figure: Inertial frame and body frame of multirotors

# Inertial Frame and Body Frame (ii)

## Origin of the body frame

- Figure 3 illustrates the frameworks used to find the dynamics models for the multi-rotors.
- The origin of the body frame is in the mass center of the multi-rotor and $z-$ axis is upwards.
- $M_1,\ M_2,\ M_3,\ M_4$ are four rotors with DC motors or the six rotors with the hexacopter.
- The dynamics models are the same for the multi-rotors, however, the implementations of the control signals will be different depending on how many rotors are used.

# Euler Angles

## Euler angles

The multi-rotor's attitude is defined by three Euler angles, namely roll about $x-$axis, pitch about $y-$axis, and yaw about $z-$axis.

## Notations

- Roll angle $\phi$: about the x body axis;
- Pitch angle $\theta$: about the y body axis;
- Yaw angle $\psi$: about the z body axis;
- The transformation sequence is $\psi \rightarrow \theta \rightarrow \phi$ in order to obtain the unique solution.

# Dynamic Model

$$\begin{bmatrix} \dot{p} \\ \dot{q} \\ \dot{r} \end{bmatrix} = \begin{bmatrix} (I_{yy} - I_{zz})qr/I_{xx} \\ (I_{zz} - I_{xx})pr/I_{yy} \\ (I_{xx} - I_{yy})pq/I_{zz} \end{bmatrix} + \begin{bmatrix} 1/I_{xx} & 0 & 0 \\ 0 & 1/I_{yy} & 0 \\ 0 & 0 & 1/I_{zz} \end{bmatrix} \begin{bmatrix} \tau_x \\ \tau_y \\ \tau_z \end{bmatrix} \quad (1)$$

# Notations and assumptions

- $I_{xx}$, $I_{yy}$ and $I_{zz}$ are the moments of inertia for the three axes in $x$, $y$, $z$ directions;
- $p$, $q$ and $r$ the body frame angular velocities in $x$, $y$, $z$ directions;
- $\tau_x$, $\tau_y$, $\tau_z$ are the corresponding torques in $x$, $y$, $z$ directions, which are the manipulated variables in the multirotor control problem.
- The quadrotor is assumed to have symmetric structure with four arms aligned with the $x-$axis and $y-$axis, and as a result there is no interaction between the torques along the three axes.
- Similar assumptions are made for the hexacopter to ensure that there is no interactions between the torques along the three axes.

# Relationships between $\phi$, $\theta$, $\psi$ and $p$, $q$, $r$

The relationships between the Euler angular velocities and the body frame angular velocities are described in the following differential equation:

$$\begin{bmatrix} \dot{\phi} \\ \dot{\theta} \\ \dot{\psi} \end{bmatrix} = \begin{bmatrix} 1 & \text{sin}(\phi)\,\text{tan}(\theta) & \text{cos}(\phi)\,\text{tan}(\theta) \\ 0 & cos(\phi) & -sin(\phi) \\ 0 & sin(\phi)/\,\text{cos}(\theta) & \text{cos}(\phi)/cos(\theta) \end{bmatrix} \begin{bmatrix} p \\ q \\ r \end{bmatrix}. \qquad (2)$$

# Outline

# Attitude Control (i)

## System Outputs

- For attitude control of a multi-rotor, the objective is to feedback control the three Euler angles so that they follow three reference signals ($\phi^*$, $\theta^*$, $\psi^*$ ).
- Therefore, the outputs of the control systems are the three Euler angles: $\phi$, $\theta$, $\psi$.

## Control variables or manipulated variables

The manipulated variables or the control signals are the three torques, $\tau_x$, $\tau_y$, $\tau_z$, along the $x$, $y$ and $z$ directions.

# Attitude Control (ii)

### Intermittent variables

The body frame angular velocities $p$, $q$ and $r$ along the $x$, $y$ and $z$ directions are the intermittent variables.

### Cascade control

- Because there are two sets of nonlinear dynamic equations, cascade control is a good choice for this nonlinear control problem.
- The body frame angular velocities $p$, $q$ and $r$ are the secondary variables because they are directly related to the manipulated variables $\tau_x$, $\tau_y$ and $\tau_z$.
- The three Euler angles, $\phi$, $\theta$, $\psi$ are the primary variables to achieve the attitude control

# Cascade Control of One Axis

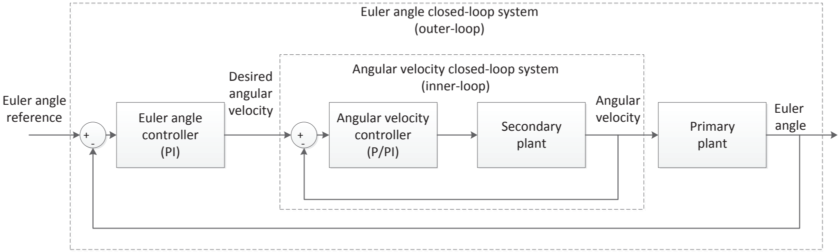


Figure: Cascade feedback control structure

# Outline

# Dynamic model (i)

$$\dot{p} = \Gamma_1 pq - \Gamma_2 qr + \frac{1}{2}\rho V_a^2 Sb \left[C_{\ell_0} + C_{\ell_{\beta_C}}\beta_C + C_{\ell_p}\frac{bp}{2V_a} + C_{\ell_r}\frac{br}{2V_a} + C_{\ell_{\delta_a}}\delta_a +$$

$$\dot{q} = \Gamma_5 pr - \Gamma_6(p^2 - r^2) + \frac{\rho V_a^2 Sc}{2I_y}\left[C_{m_0} + C_{m_\alpha} + C_{m_q}\frac{cq}{2V_a} + C_{m_{\delta_e}}\delta_e\right] \tag{3}$$

$$\dot{r} = \Gamma_7 pq - \Gamma_1 qr + \frac{1}{2}\rho V_a^2 Sb \left[C_{n_0} + C_{n_{\beta_C}}\beta_C + C_{n_p}\frac{bp}{2V_a} + C_{n_r}\frac{br}{2V_a} + C_{n_{\delta_a}}\delta_a$$

where $p, q$ and $r$ are angular rates in the body frame and the control surface inputs are $\delta_a$, $\delta_e$ and $\delta_r$.

# Dynamic model (ii)

The relationships between the body frame angular rates and the Euler angular rates are described in the following equation:

$$\begin{bmatrix} \dot{\phi} \\ \dot{\theta} \\ \dot{\psi} \end{bmatrix} = \begin{bmatrix} 1 & sin(\phi)tan(\theta) & cos(\phi)tan(\theta) \\ 0 & cos(\phi) & -sin(\phi) \\ 0 & sin(\phi)sec(\theta) & cos(\phi)sec(\theta) \end{bmatrix} \begin{bmatrix} p \\ q \\ r \end{bmatrix} \tag{4}$$

# Attitude Control of Fixed-wing Aircraft

## System Outputs

- For attitude control of a fixed-wing aircraft, the objective is to feedback control the three Euler angles so that they follow three reference signals ($\phi^*$, $\theta^*$, $\psi^*$ ).
- Therefore, the outputs of the control systems are the three Euler angles: $\phi$, $\theta$, $\psi$.

## Control variables or manipulated variables

The manipulated variables or the control signals are the three control surface inputs, $\delta_a$ (x-axis), $\delta_e$ (y-axis), $\delta_r$ (z-axis).

## Cascade Control Structure

The control structure is identical to the multi-rotor UAV structure except that the manipulated variables are the three control surface inputs ($\delta_a$, $\delta_e$, $\delta_r$).

# Discussions of Cascade Control

- The dynamics of three axes are almost decoupled, thus PI controllers are designed for each axis separately.
- The inner-loop controller (also called secondary controller) is to control inner-loop (secondary) plant, where its reference signal is the desired angular velocity that is also the control signal generated from the outer-loop (primary) controller.
- For the cascade control system, the primary objective is to control the outer-loop (primary) plant to achieve desired closed-loop performance.

# Outline

# Actuators

- The torques $\tau_x$, $\tau_y$ and $\tau_z$ in the body frame are the control signals.
- The four DC motors are the actuators that will realize the control signals calculated using the controllers.
- The DC motors have dynamics and we need to consider them in the control system design.
- The challenge is how to realize the calculated torques from the cascade control system using the DC motors.

# The Actuator Dynamics (i)

In quadrotor control, the torques $\tau_x$, $\tau_y$ and $\tau_z$ in the body frame are generated by the differences in rotor thrusts.

## Rotor thrusts

The upward thrust produced by each rotor is

$$T_i = b_t \omega_i^2, \quad i = 1, 2, 3, 4.$$

The total thrust is, hence,

$$T = \sum T_i$$

where $b_t$ is the thrust constant determined by air density, the length of the blade and the blade radius, $\omega_i$ is the *ith* rotor's angular speed.

# The Actuator Dynamics (ii)

### Torques ($\tau_x$, $\tau_y$)

The torques about quadrotor's $x-$axis and $y-$axis are

$$\tau_x = d_{mm}(T_4 - T_2) = d_{mm}b_t(\omega_4^2 - \omega_2^2) \quad (5)$$
$$\tau_y = d_{mm}(T_3 - T_1) = d_{mm}b_t(\omega_3^2 - \omega_1^2), \quad (6)$$

### Torque $\tau_z$

The torque applied to each propeller by the motor is opposed by aerodynamic drag and the total reaction torque about the z-axis is

$$\tau_z = k_d({\omega_1}^2 + {\omega_3}^2 - {\omega_2}^2 - {\omega_4}^2), \quad (7)$$

where $d_{mm}$ is the distance from the motor to the mass center, and $k_d$ is a drag constant determined by the same factors as $b_t$.

# The Actuator Dynamics in Matrix Form

The relationship between torques, thrust and rotors' angular speed is given in the following matrix form:

$$\begin{bmatrix} \omega_1^2 \\ \omega_2^2 \\ \omega_3^2 \\ \omega_4^2 \end{bmatrix} = \begin{bmatrix} 1/4b_t & 0 & -1/2d_{mm}b_t & -1/4k_d \\ 1/4b_t & -1/2d_{mm}b_t & 0 & 1/4k_d \\ 1/4b_t & 0 & 1/2d_{mm}b_t & -1/4k_d \\ 1/4b_t & 1/2d_{mm}b_t & 0 & 1/4k_d \end{bmatrix} \begin{bmatrix} T \\ \tau_x \\ \tau_y \\ \tau_z \end{bmatrix} \tag{8}$$

Because the altitude of the UAV is not controlled in this case, the total thrust is manually set by the operator.

# Implementation of Control Signal

- From (8), once the manipulated variables $T$, $\tau_x$, $\tau_y$,$\tau_z$ are decided by the cascade feedback controllers, the velocities of motors will be uniquely determined.
- The rotors acting as the actuators in this UAV control application will implement the control actions determined by $T$, $\tau_x$, $\tau_y$, $\tau_z$, through their reference signals $\omega_1$, $\omega_2$ $\omega_3$ and $\omega_4$.
- However, because the velocities of the DC motors are not measured and can not directly changed, they could not be chosen as the implementation of the control signals.
- Instead, the duty cycles of PWM signals regulating the DC voltages of the motors are used for the actual implementation of the control signals.

# DC Motor Dynamics

- The DC motor dynamics are approximated by a first-order transfer function with time delay:

$$\frac{\Omega_i(s)}{V_i(s)} = \frac{r_{wv} e^{-d_m s}}{\epsilon_m s + 1}, \tag{9}$$

- $V_i(s)$ is the Laplace transform of the armature voltage to the *ith* motor, $\epsilon_m$ is the time constant, $d_m$ is the time delay, and $r_{wv}$ is the steady-state gain.

# Duty Cycle of the Motor

How do we change the armature voltage?

- The armature voltage $v_i$ is changed by manipulating the duty cycle of the PWM signal of each motor drive.
- The relationship between the motor armature voltage and the PWM duty cycle is

$$v_i = d_i V_{bat}, \tag{10}$$

  where $d_i$ is the PWM signal duty cycle of the *ith* DC motor drive and $V_{bat}$ is the battery voltage assumed to be constant.

# Actuator Dynamics

$$\frac{\Omega_i(s)}{D_{cycle-i}(s)} = \frac{V_{bat} r_{wv} e^{-d_m s}}{\epsilon_m s + 1} \tag{11}$$

$D_{cycle-i}(s)$ is Laplace transform of the PWM signal duty cycle of the *ith* DC motor drive.

# Outline

# Auto-tuner Mechanism

## Relay Feedback Control

- A proportional controller with known gain $K_T$ is used to stabilize the integrating system;
- a relay feedback control system is deployed for the output of the closed-loop system.

## Block diagram

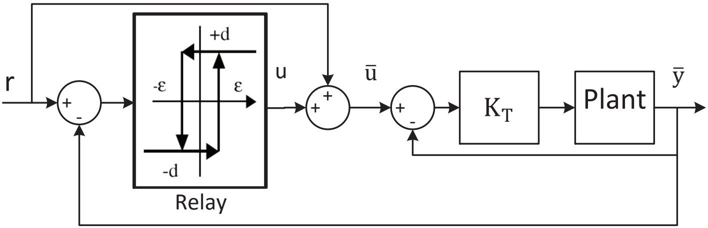


Figure: Block diagram of relay feedback control.

# The Input and Output Signals

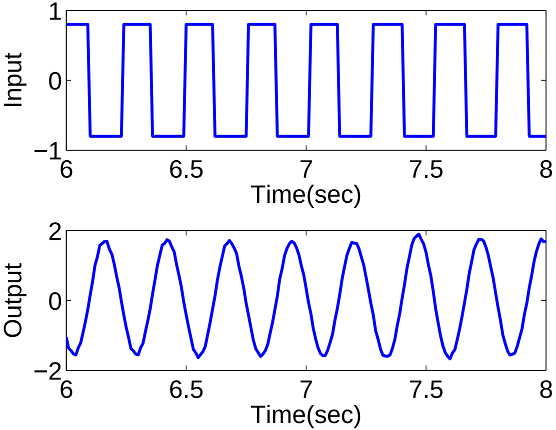


Figure: Relay feedback control signals from inner-loop system: top figure input signal; bottom figure output signal.

# The Characteristics of Relay Control

- Assume that the period of the oscillation is $T$.
- The frequency of the periodic signal $\bar{u}(t)$, denoting by $\omega_1 = \frac{2\pi}{N\Delta t}$, approximately corresponds to the frequency illustrated on the Nyquist curve shown in Figure 7.

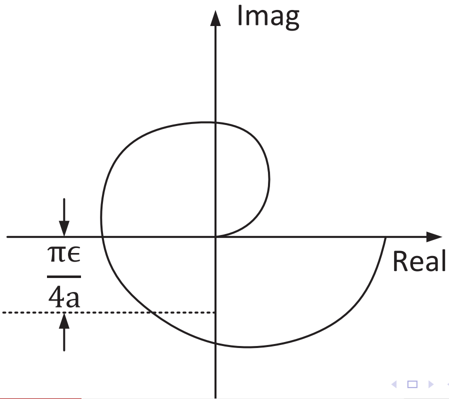

# Characteristics of Periodic Signals

- For a period $T$, the Fourier series expansion of the periodic input signal $u(t)$, is expressed as

$$u(t) = \frac{4a}{\pi}(\sin\frac{2\pi}{T}t + \frac{1}{3}\sin\frac{6\pi}{T}t + \frac{1}{5}\sin\frac{10\pi}{T}t + \ldots) \tag{12}$$

- By choosing sampling interval $\Delta t$ and the number of samples within one period $N = \frac{T}{\Delta t}$, the discretized input signal $u(t)$ at sampling instant $t_k = k\Delta t$ becomes

$$u(k) = \frac{4a}{\pi}(\sin\frac{2\pi k}{N} + \frac{1}{3}\sin\frac{6\pi k}{N} + \frac{1}{5}\sin\frac{10\pi k}{N} + \ldots) \tag{13}$$

# Estimation of $T(j\omega_1)$ using Fast Fourier Transform

- The simplest way to estimate the frequency response of the system under relay feedback is to use Fast Fourier Transform.
- Assuming that the data length is $L$, the Fourier transform of the input signal $u(k)$, $k = 1, 2, \ldots, L$, is

$$U(n) = \frac{1}{L}\sum_{k=1}^{L} u(k)e^{-j\frac{2\pi(k-1)(n-1)}{L}} \tag{14}$$

and the corresponding Fourier transform of the output is

$$Y(n) = \frac{1}{L}\sum_{k=1}^{L} y(k)e^{-j\frac{2\pi(k-1)(n-1)}{L}} \tag{15}$$

where $n = 1,\ 2,\ 3,\ \ldots,\ L$.

- From both (14) and (15), with the definition of Fourier transform, the corresponding discrete frequency $\omega_d$ is defined from 0 to $\frac{2\pi(L-1)}{L}$ with an incremental of $\frac{2\pi}{L}$.

# Example: Input and Output Data

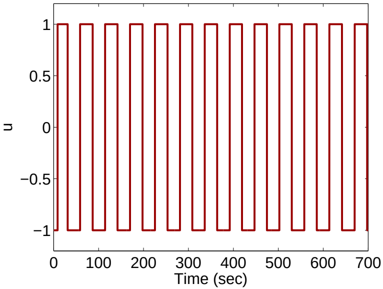


(a) Input data

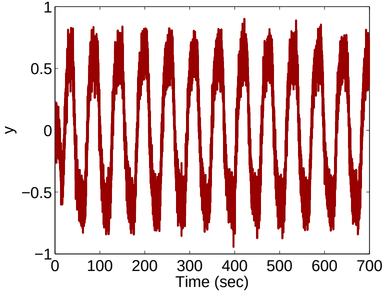


(b) Output data

# Fourier Transform (1)

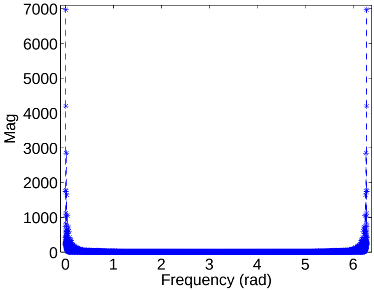


(c) Fourier transform $U(e^{j\omega_d})$

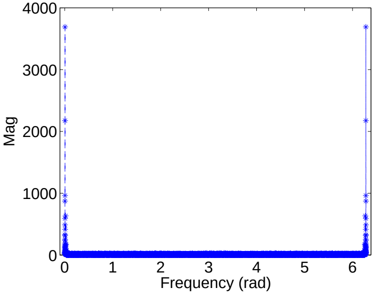


(d) Fourier transform $Y(e^{j\omega_d})$

# Fourier Transform (2)

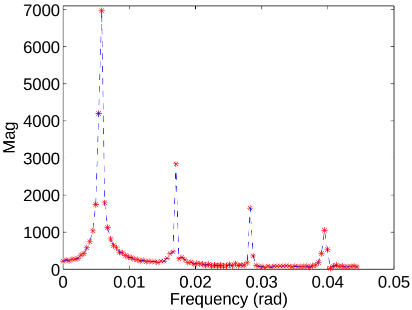


(e) Fourier transform $U(e^{j\omega_d})$, $0 \leq \omega_d \leq 0.045$

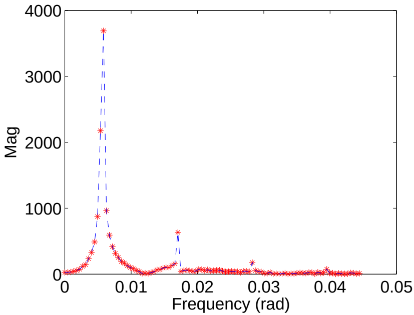


(f) Fourier transform $Y(e^{j\omega_d})$, $0 \leq \omega_d \leq 0.045$

# Example (iii)

- Locating the fundamental frequency of the relay signal as the maximum value of $U(e^{j\omega_d})$, Identify the peaks of $U(e^{j\omega_d})$ as the 14*th* sample, which is the frequency at $\omega_d = \frac{2*\pi(14-1)}{L}$, $L = 14001$.
- The estimation of the frequency response of the system is then given by

$$T(14) = Y(14)/U(14) = -0.0040 - 0.5293i$$

- The second peak is identified at the 39*th* sample, which is the frequency at $\omega_d = \frac{2*\pi(39-1)}{L}$, $T = -0.1081 + 0.1950i$. The third peak is identified at 64*th* sample, which is the frequency at $\omega_d = \frac{2*\pi(64-1)}{L}$, $T = 0.1054 - 0.0151i$.

# Comparative Results

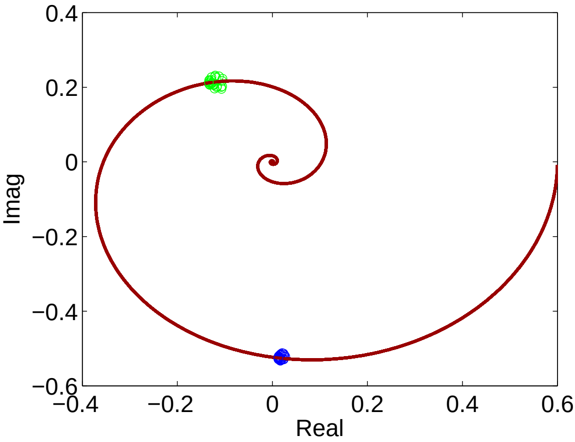


Figure: Comparison between the estimated frequency points with the actual frequency response.

# Outline

# Integrator Plus Time Delay Model

- For an integrating plus time delay system, a single frequency is sufficient to determine its gain $K_p$ and time delay $d$.
- The approximate model of an integrating system is assumed to be of the following form:

$$G_p(s) = \frac{K_p e^{-ds}}{s} \tag{16}$$

# Finding the Parameters (i)

- Letting the frequency response of the integrator plus delay model (16) be equal to the estimated $G_p(j\omega_1)$ leads to

$$\frac{K_p e^{-jd\omega_1}}{j\omega_1} = G_p(j\omega_1) \tag{17}$$

- Equating the magnitudes on both side of (17) gives

$$K_p = \omega_1 |G_p(j\omega_1)| \tag{18}$$

where $|e^{-jd\omega_1}| = 1$.

# Finding the Parameters (ii)

- Additionally, from (17), the following relationship holds:

$$e^{-jd\omega_1} = \frac{j\omega_1 G_p(j\omega_1)}{K_p}$$

- This gives the estimate of time delay as

$$d = -\frac{1}{\omega_1} tan^{-1} \frac{Imag(jG_p(j\omega_1))}{Real(jG_p(j\omega_1))} \tag{19}$$

# PID Controller Design

The parameter $\beta$ is the scaling factor for the desired closed-loop time constant, which is defined as

$$\tau_{cl} = \beta d$$

$$K_c = \frac{\hat{K}_c}{dK_p}$$

$$\tau_I = d\hat{\tau}_I$$

$$\tau_D = d\hat{\tau}_D$$

# Normalized PID Parameters (i)

Table: Normalized PID controller parameters ($\xi = 0.707$)

| | $0.7 \leq \beta \leq 1$ | $1 < \beta \leq 11$ |
|---|---|---|
| $\hat{K}_c$ | $\frac{1}{0.3280\beta^2+0.0786\beta+0.6442}$ | $\frac{1}{0.7184\beta+0.3661}$ |
| $\hat{\tau}_I$ | $-3.7845\beta^2 + 10.2044\beta - 4.0298$ | $1.3970\beta + 1.2271$ |
| $\hat{\tau}_D$ | $\frac{1}{-1.9064\beta^2+6.1545\beta-1.5875}$ | $\frac{1}{1.4275\beta+1.6450}$ |

# Outline

# Components

| Function | Model |
|---|---|
| DC motor drive | DRV8833 Dual Motor Driver Carrier |
| Sensor board | MPU6050 |
| Micro processor | STM32F103C8T6 |
| RC receiver | WFLY065 |
| DC motor | 820 Coreless Motor |
| RC transmitter | WFT06X-A |
| Data logger | SparkFun OpenLog |

Table: quadrotor hardware list

# Experimental Data

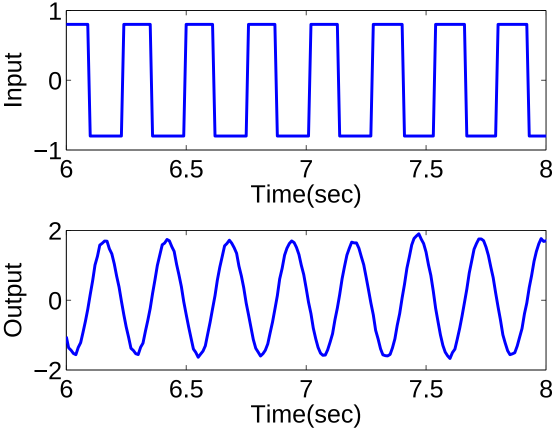


Figure: Relay feedback control signals from inner-loop system: top figure input signal; bottom figure output signal.

# Closed-loop Control Results

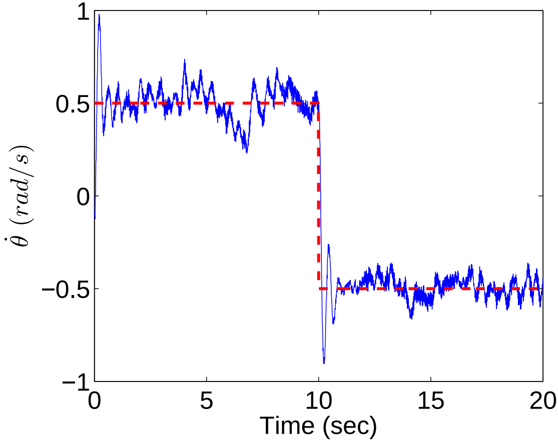


Figure: Inner-loop step response in closed-loop control. Dashed line: reference signal; solid line: output.

# Auto-tuning of Primary PI Controller

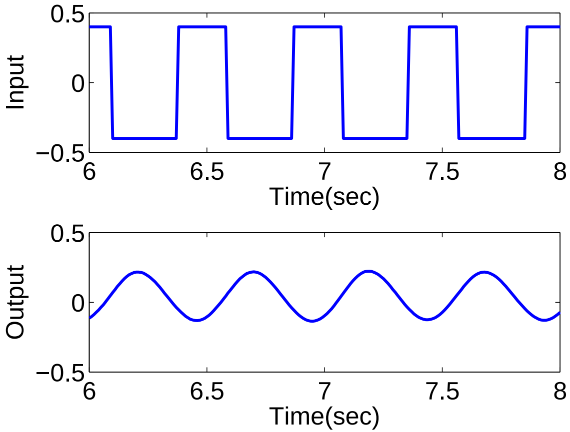


Figure: Relay feedback control signals from outer-loop system: top figure input signal; bottom figure output signal.

# Closed-loop Control Results

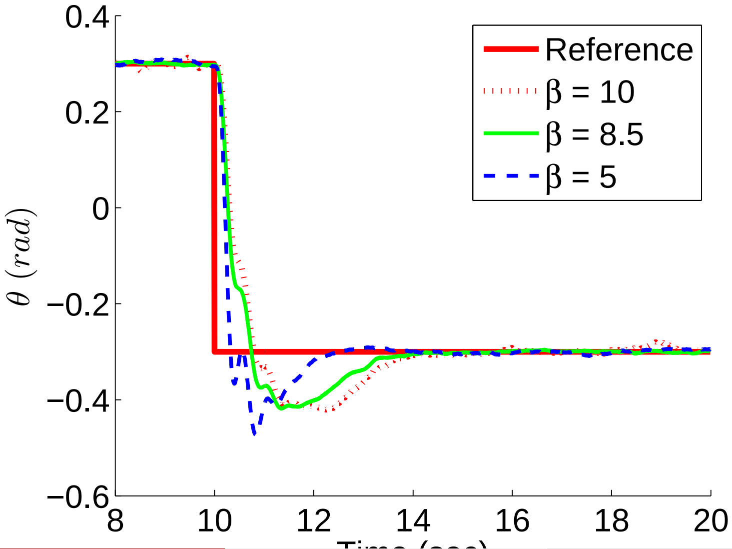

# Outline

# Components

Table: Flight controller and avionic components

| Components | Descriptions |
|---|---|
| Airframe | Turnigy Talon Hexacopter |
| Microprocessor | ATMega2560 |
| Inertial measurement unit | MPU6050 |
| Electronic speed controllers | Turnigy 25A Speed Controller |
| Brushless DC motors | NTM Prop Drive 28-26 235W |
| Propellers | 10x4.5 SF Props |
| RC Receiver | OrangeRX R815X 2.4Ghz receiver |
| RC Transmitter | Turnigy 9XR PRO transmitter |
| Datalogger | CleanFlight Blackbox Datalogger |

# Relay experimental data

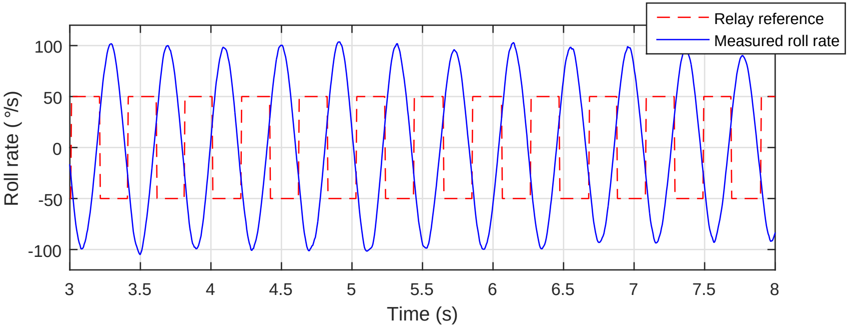


Figure: Inner loop relay test result. $K_T = 0.3$, $R_a = 50^\circ/s$, $\epsilon = 30^\circ/s$

# Controller parameters

**Controller parameters found for inner-loop**

$K_c = 0.33, \tau_I = 0.26$ and $\tau_D = 0.03$

**Controller parameters found for outer-loop**

$K_c = 3.3$, $\tau_I = 0.63$ and $\tau_D = 0.013$.

# Outdoor flight testing

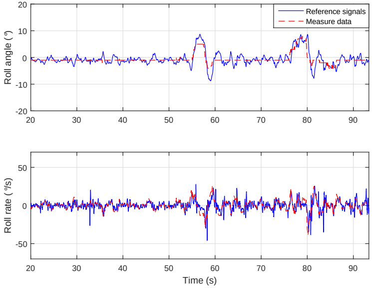


(a) Roll control:top-angle,bottom- rate

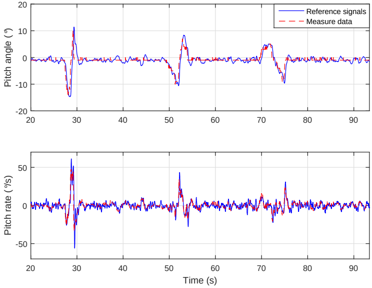


(b) Pitch control:top-angle,bottom- rate

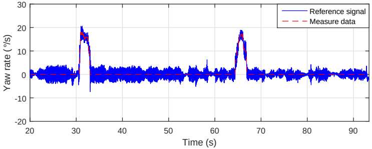


(c) Yaw control results

Figure: Experimental testing results. Key- red dashed lines: the reference signals; blue solid lines: the measured data

# Outline

Table: Fixed-wing UAV Specifications

| Description | Details |
|---|---|
| Airframe | Slick 360 |
| Airfoil | NACA0012 |
| Wing span | $0.490m$ |
| Fuselage length | $0.421m$ |
| Wing area | $0.44m^2$ |
| Average chord | $0.0885m$ |
| Weight | $130g$ |
| Cruise speed | $10m/s$ |

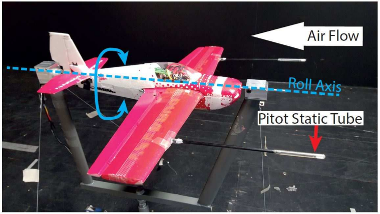


Figure: The fixed-wing UAV on the roll test rig

# Relay experimental data

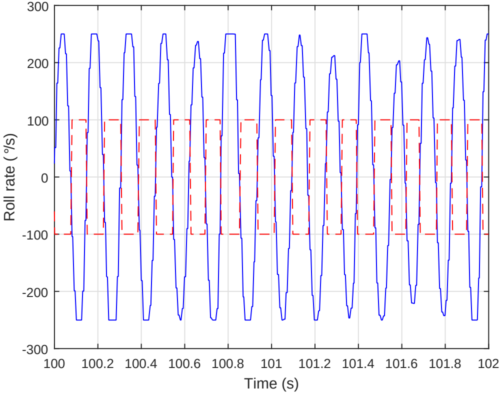


Figure: Inner loop relay experiment: red (dashed) = reference signal, blue (solid) = measured data

# Inner-loop control testing results

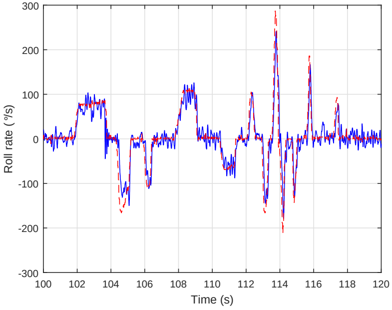


(a) Angular rate tracking

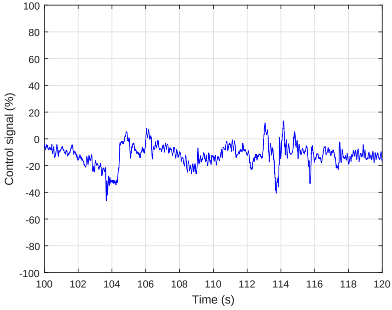


(b) Control signal $\delta_a$

Figure: Inner loop experimental validation: red (dashed) = reference signal; blue (solid) = measured data

# Outer-loop relay control

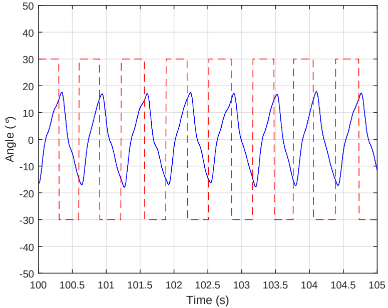


(a) Angular loop

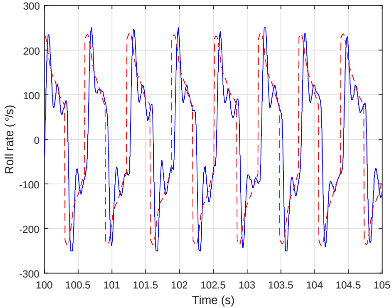


(b) Angular rate loop

Figure: Outer loop relay experiment: red (dashed)- reference signal; blue (solid)- measured data

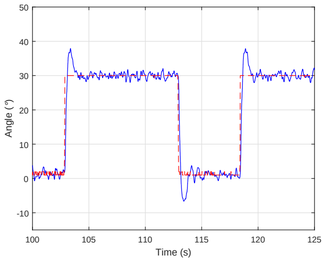


(a) Angular tracking

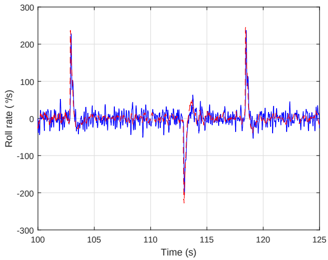


(b) Angular rate tracking

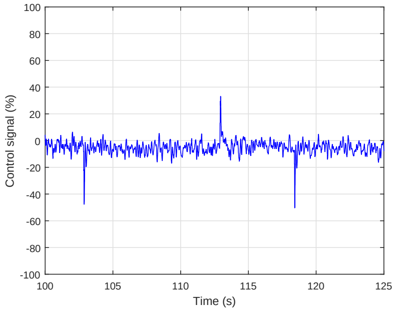


(c) Control signal $\delta_a$

# Summary

- Conduct a relay control experiment to obtain the set of input and output data;
- Estimation of the plant frequency information;
- Find the integrating plus delay model;
- Find the PID controller parameters based on the delay and gain.